Advantage of Increasing the Number of Airgap Surfaces in Synchronous Linear Actuators

Pierre-Emmanuel Cavarec, Hamid Ben Ahmed, Bernard Multon, Laurent Prevond

Advantage of Increasing the Number of Airgap Surfaces in Synchronous Linear Actuators

*P.E. Cavarec, H. Ben Ahmed, B. Multon, L. Prévond**

Laboratoire d'Electricité, Signaux et Robotique (LESiR, ESA CNRS 8029)
ENS de Cachan - Brittany Branch
Campus de Ker Lann, 35170 BRUZ

* E.N.S. de Cachan 61 avenue du president Wilson 94235 Cachan

e-mail: cavarec@bretagne.ens-cachan.fr

Abstract. This paper presents an realistic comparison of several electromagnetic architectures for high force density actuators. Firstly a simple classification of synchronous actuators is presented. Four equivalent architectures are chosen and modelized by saturable reluctance schemes. For each size and each architecture, dimensions are optimized in order to maximize the force-volume ratio. This optimization is done with fixed mecanical airgap. A simple thermical model is used. Results shows that the optimal number of airgaps increase with the dimensions. Moreover, Global coil architecture performances increase faster than other architectures.
Several examples of global coil multiairgaps actuators are presented in order to illustrated the theoretical result.

I. INTRODUCTION

It is quite frequent for direct-drive applications to require high force density actuators (e.g. electrical jacks, robot arms, integrated wheel-motors). In general, whenever torques or forces need to be produced in a minimal size, either the number of poles is increased or the polar step is reduced in order to minimize the quantity of magnetic circuit; however, the physical limitations of airgap magnetic shear stress can not be overcome. This stress gets limited by means of both the airgap induction and the magnetic field density in the armature currents. Airgap induction is limited by the saturation of ferromagnetic materials, and the field is limited by heating and/or the demagnetization of eventual magnets. The attainable maximum values of the airgap magnetic shear stress rarely exceed 10 N/cm². An actuator can thereby be summarized as a system for producing magnetic fields that interact inside an airgap where magnetic stress is generated.
Another approach, conceived some twenty years ago [1,2] yet still rather undeveloped due to its conceptual complexity, consists of splitting the active zone so as to increase the airgap surfaces, giving rise to what are called "multi-airgap structures".
In this paper, we will start by proposing a classification of synchronous machine topologies. Next, we will draw a comparison of the evolution of several architectures in an effort to highlight the value of global coil multi-airgap structures. An example of a specific configuration will be presented afterwards.

II. DIFFERENT SYNCHROUNOUS TOPOLOGIES

Among the set of synchronous machines, a distinction can be drawn between the following:

- excited machines (with either permanent magnets or coiled excitation); and
- Non-excited machines (with variable reluctance).

Moreover, four types of coupling can be distinguished, depending on the nature and shape of the magnetic field (see Fig. 1):

- polar coupling: rotational field, heteropolar field motor;
- toothed Vernier coupling: rotational field, homopolar field motor;
- toothed heteropolar coupling: pulsating field, heteropolar field motor; and
- Toothed homopolar coupling: pulsating field, homopolar field motor.

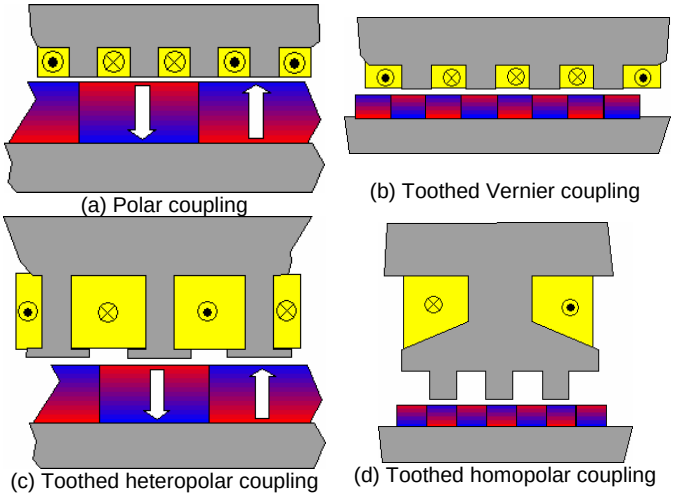

Fig. 1: Range of couplings on topologies

It should also be noted that with respect to displacement, two basic flux configurations are possible and a hybrid or classical one:

P.E. CAVAREC, H. BEN AHMED, B. MULTON, L. PRÉVOND, « Advantage of Increasing the Number of Airgap Surfaces in Synchronous Linear Actuators », Electromotion'01 Intern. Conf. Bologna, 19-20 June 2001, pp.251-256.

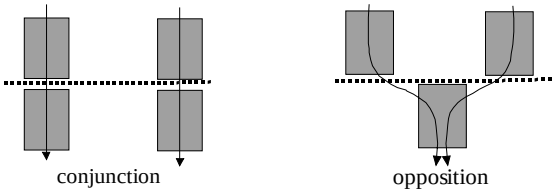

Fig. 2a: Transverse flux reluctance actuator

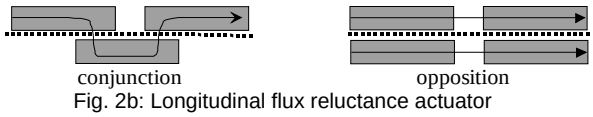

Fig. 2b: Longitudinal flux reluctance actuator

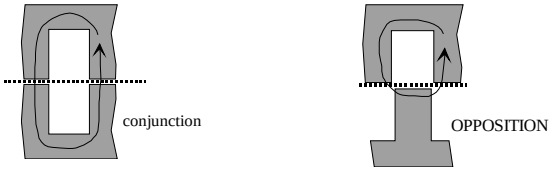

Fig 2c Hybrid or classical flux reluctance actuator

III. METHODOLOGY OF COMPARISON OF THE MULTIAIRGAP STRUCTURES

The so-called "classical" structures, featuring variable reluctance and/or permanent magnets generate maximum force density on the order of 300 N/dm^3, for primarily heat-related reasons.
The increase in force-volume ratio requieres expanding the number of airgap surfaces.
In order to emphasize the advantages of this multiplication step as well as its application conditions, we have examined, as a means of application, the scale effects on four topologies of linear "multi-stack" actuators with permanent magnets and a toothed homopolar or heteropolar coupling (like Figs. 1c and 1d).

III 1 Machine architectures

The four architectures included in this study were the following:

- So-called "basic" single-airgap architecture (see Fig. 3a). In this configuration, the increase in stress density necessitates optimizing just the architecture's geometry;
- So-called "multi-motor" architecture (Fig. 3b), corresponding to the superposition of several basic architectures. In this configuration, the increase in stress density necessitates the optimization of both the geometry and the number of motors [6];
- So-called "split coil multi-airgap" architecture (Fig. 3c), corresponding to the preceding configuration yet with shared flux return circuits. This configuration is set up for normal flux (Fig. 2a).
- So-called "global coil multi-airgap" architecture, in which the coil magnetizes all airgap surfaces. This configuration is set up for longitudinal flux (like Fig. 2b).

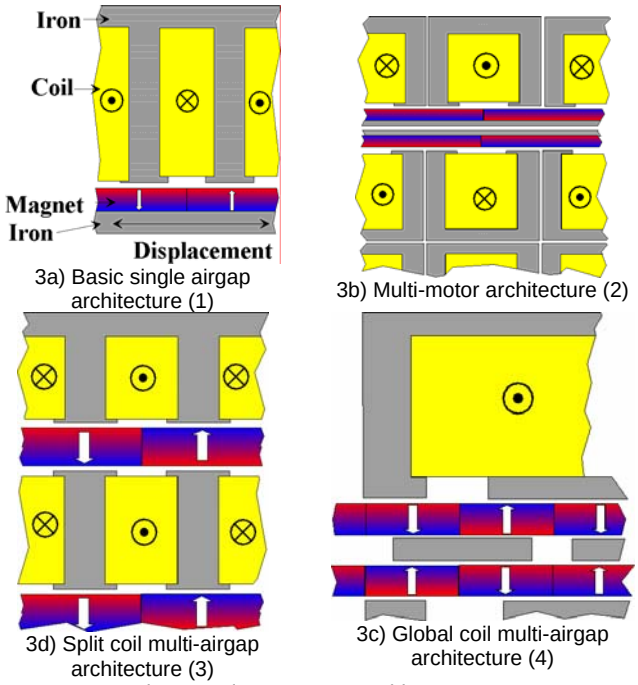

Fig. 3: Various actuator architectures

III 2 Design methodology

The aim of this calculation is a comparison between several architectures. That why we are more interested by the evolution of the performance than the value of the performance itself. The important point is to take exactly le same calculation model for the different dimensions and the deferent architectures
Calculating the performance of the structures described above is carried out using a computation of the global energy conversion stoke (i.e. the virtual work method).

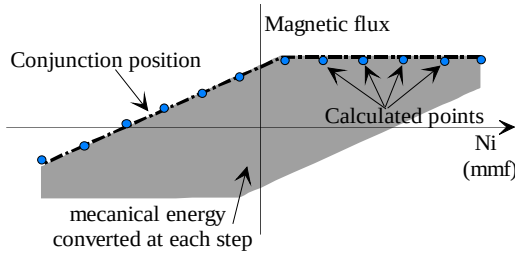

Fig 4: Global energy conversion cycle

In such a condition, simple model as saturable reluctance model can give good solutions in a short time
In the case of architecture types 1, 2 and 3 above, the energy converted by one cycle is equal to the energy converted by a single "motor" multiplied by the number of "motors" constituting the structure.

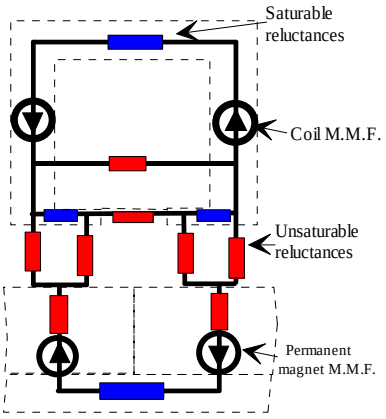

Fig 5 a): Type 1,2,3, parameterable reluctant model

In the architecture type 4, the coil is distributed on each elementary cell:

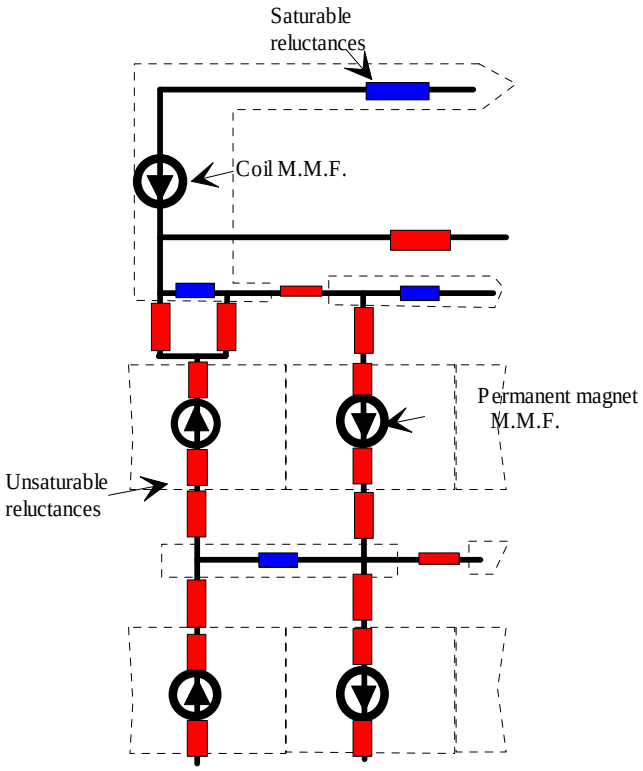

Fig 5 b): Type 4 parametrable reluctant model

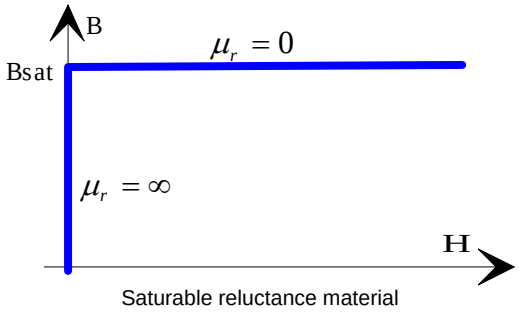

III 3 Condition of comparison

To highlight the advantage of multiplying the number of airgap surfaces, a comparison was drawn between force densities at the same volume and several scales. This comparison has been conducted under the following conditions:

- a constant mechanical airgap length ;
- a cubic, three phases overall actuators shape. It means that a complete motor is made of three independents phases.

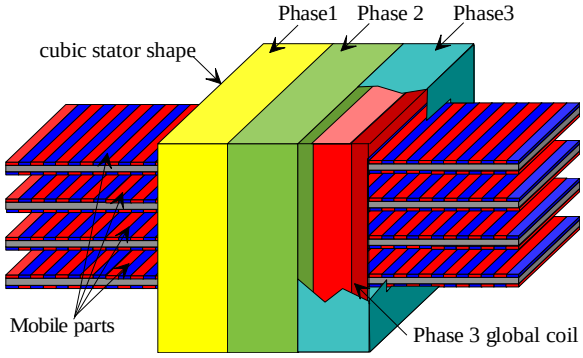

Fig 6: Global coil, cubic tree phases overall shape, actuator

- constant heating. Heat exchange through the winding surface is presumed, at a given level of heating, which imposes copper losses proportional to this exchange surface (see Fig. 7).

Fig. 7: Cooling surface of the winding

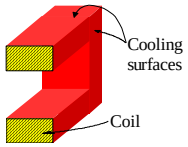

The thermical model is resume by the equations:

$$P_{Cu} = R.I_{eff}^2 = \rho.V_{cu}.J^2 = \alpha.S_{cooling}.\Delta T$$

With:

$S_{cooling}$ the exterior surface of the coil

α the surfacic exhange heat coefficient (W.m².K)

ρ the copper resistivity ($\Omega.m$)

ΔT

III 4 THE OPTIMISATION ALGORITHM

The aim of the search algorithm is to optimize each of the different architectures. In those conditions, comparisons are realistic.

The geometric optimization is difficult because of the number of free parameters (up to 6). Hence, classical optimization algorithms can't be efficient because of local optimums.

We have used a genetic algorithm. This algorithm is based on the natural selection process.

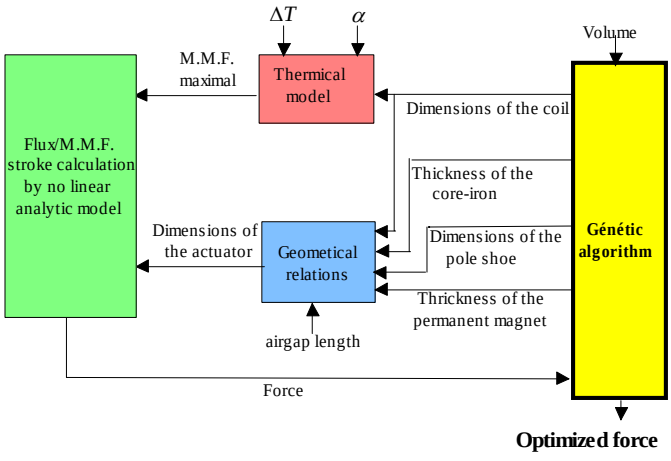

Global scheme of the genetic algorithm

IV. RESULTS OF THE COMPARISONS

Several comparisons have been made on the multiairgap structures. Firstly, the comparison of the optimal number of airgaps surfaces for different outsides volumes. Then the comparison of the force-volume density

IV 1 COMPARISON OF THE OPTIMAL NUMBER OF AIRGAPS

The results obtained for the four types of architecture discussed earlier, subject to the computation conditions listed below, have been provided in Figure 8:

- Airgap length g = 1 mm;
- maximum temperature rise ΔT = 100°C;
- square wave current supply;
- heat dissipation α = 10 W/m².°C (free air convection);
- P.M. flux density B_r = 1 T; and

demagnetization limit H_c = 1,000 kA/m.

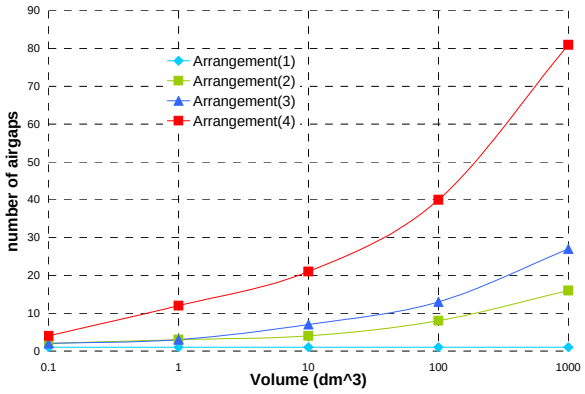

Fig. 8: Evolution in the optimal number of airgap surfaces

We can see that some arrangements are well adapted to the multiplying of the number of airgaps.
The fewer places the coil takes, the more numerous the airgaps are. That why arrangement (4) (with global coil) are well adapted to the increase of the number of airgaps.

IV 2 COMPARISON OF THE VOLUMIQUE FORCE

With the same conditions, we can compare the force for several volumes. We can see that all architectures increase there performance

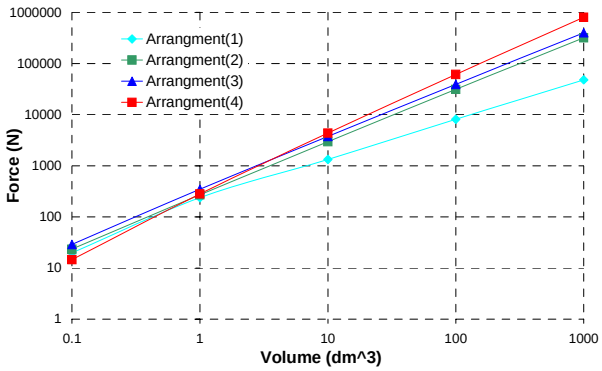

If we divide the force by the volume, the force-volume ratio gives the evolution:

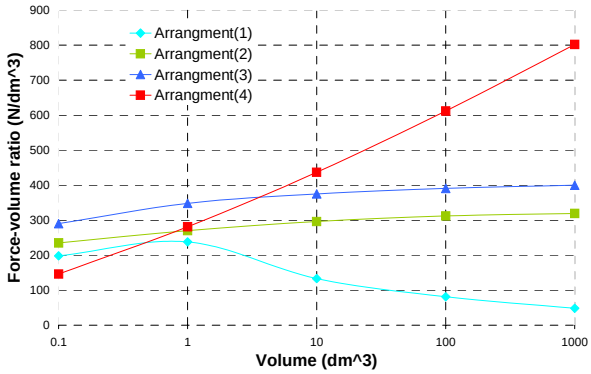

Fig. 9a): Evolution in the volume-force ratio as a function of volume (g=1mm, α =10W/m²)

These results thereby highlight that multiplying the number of airgap surfaces merely allows for architecture classifications (2) (see Fig. 3a) and (3) (Fig. 3c) to remain at the optimal level of force-volume ratio, yet with a more moderate value (approx. 400 N/liter). In the case of architecture (4) (Fig. 3d), the architecture is penalized in small dimension because it have a four magnetic airgaps per elementary cell. However, this multiplication operation has enabled significantly increasing the force-volume ratio for important volume (to above 800 N/liter for 1m³) (Fig. 8a) thanks to an even greater extent as the number of surfaces rises (Fig. 8b). This architecture became interesting for volume around 5 liters.
Architecture (1) (Fig. 3a), on the other hand, is adversely affected by the constraint of respecting a cubic shape. Its force increases more slowly than its volume. A flatter shape would be better adapted to this particular architecture.
Moreover, the demagnetizations limit is reached

IV 3 Comparison of the volumique force with smaller airgap

In this comparison, we have optimised the same architectures with reduced airgaps lenght of half (i.e. 0.5 mm).

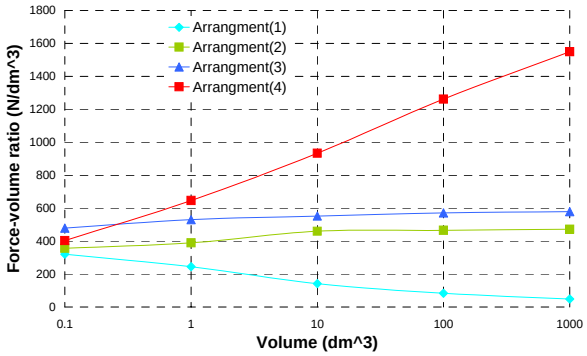

Fig. 9b): Evolution in the volume-force ratio as a function of volume with halp airgap (g=0.5 mm, α =10W/m²)

We can see that all multiairgap architectures have their force-volume ratio increased. However, the architecture (4) became interesting for smaller volumes (around half litter). The airgap lenght dimension is the key of the performance increasing in multiairgap global coil topologies

IV 4 Comparison of the volumique force with better cooling conditions

The last comparison increase the heat dissipation to α =40W/m² . It means that we can double the current intensity.

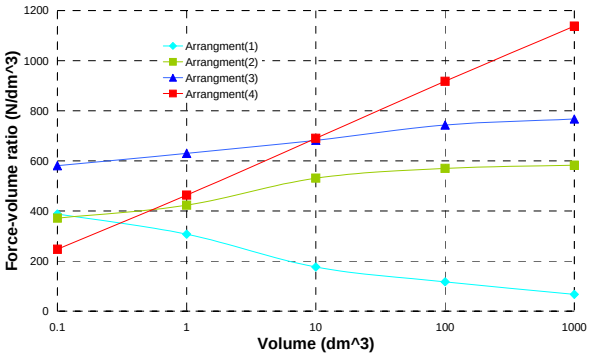

Fig. 9c): Evolution in the volume-force ratio as a function of volume with better cooling conditions (g=1mm, α =40W/m²)

Once again, all architectures increase their performances. Results show that architecture (4) is still interesting but for bigger volumes. It can be explained by the fact that global coil give an advantage to architecture (4) if the heat dissipation is limited. When the heat dissipation is enhanced, architecture (4) became less efficieny (For all architectures, the copper volume is less important, so, the advandage of architecture (4) is less efficiency).

V. CASE OF ROTATIVE ACTUATORS

Linear actuators and rotative actuators are very similar. We can transform one linear topology to a rotative one by creating a rotation axis.

In a planar motor three directions of rotation may be chosen. This three directions are related to the three directions of space.

- The first axis, parallel to the displacement direction, gives a tubular linear motor. Fig10b)
- The second axis gives a cylindrical rotative motors Fig 10c)
- The third axis gives discoid rotative motors Fig10d)

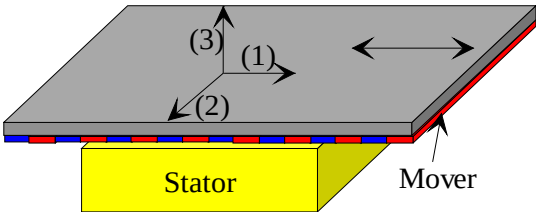

Fig 10a)Linear architecture

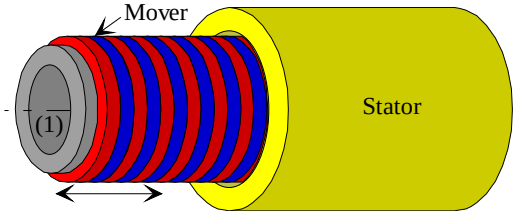

Fig 10b): Tubular linear motor

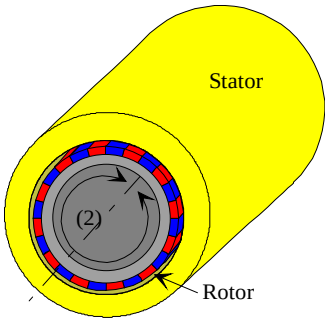

Fig 10c):Cylindrical architecture

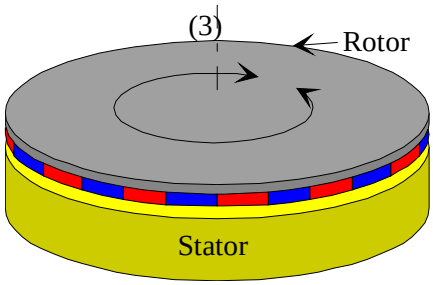

Fig 10d): Discoid architecture

We can see that all this architectures have the same basic behavior.

However, it is clear that multiairgaps cylindrical actuator would have been mechanically very complicated. That why, we can say that a rotative multiairgap actuator have to be discoid.

It would be interesting to extend the linear actuators results to rotative actuators. Hence, there are three main differences between a linear actuator and a rotative one:

- The output value is no more the force-volume ratio but the torque-volume ratio. This mean that the distance between the cell and the rotation axis became a fundamental value in the optimization.
- In discoid architectures, the optimal step can't be maintained in all the volume. The optimization became global and we can't have anymore an "optimal cell". A more exact study has to be made.
- The rotor has to be maintaining to the axis. We can't use the same architecture of global coil around the active part. That why, in rotative multiairgap actuator, longitudinal flux actuator must have a induction coil in another place

VI. EXAMPLES OF GLOBAL COIL MULTI-AIRGAP ARCHITECTURE

As a means of verifying the theoretical results as well as the principle of multiplying the number of airgap surfaces, we have developed several global coil multi-airgap linear

VI 2 A variable reluctance linear motor

The second architecture is a longitudinal flux reluctance linear actuator. The architecture has 26 airgaps. The stator and the mover are made by magnetic strips. Those strips are rubbing on each other. The active part weigh around 2kg. The stroke is 40 mm and the magnetic step of 6mm.

The force in normal cooling conditions is 1200N. This exceptional force-volume ratio is obtained thanks to numerous airgaps.

This exceptional force-weight ratio have been possible thanks to an important splitting of the active part and a contact guides.

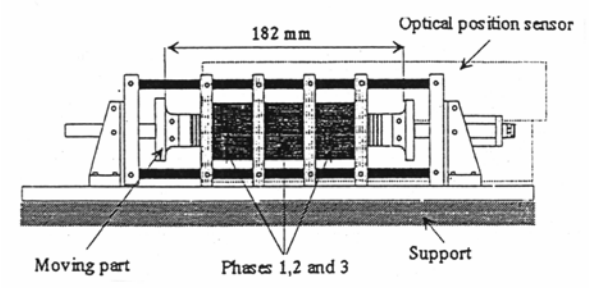

Figure 16a) A multiairgaps variable reluctance motor

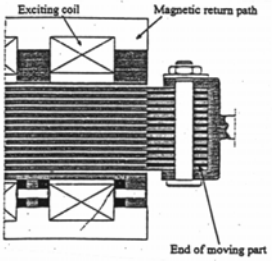

Figure 16b) actuator extremity

VI 3 The permanentmagnet star structure

The last example of such a structure is displayed in Figure 17 and 18.

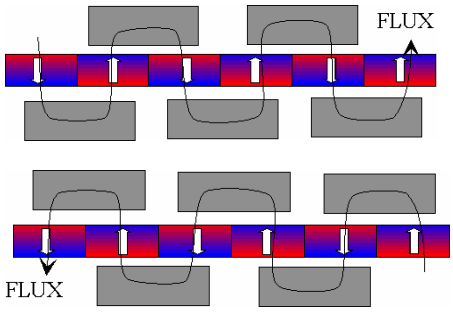

Fig 17a) positive conjunction

Fig 17b) Negative conjunction

Figure 17 Elementary cell of the multiairgaps actuator

This actuator features permanent magnets of NdFeB type with an induction of 0.65 T and a longitudinal field [5]. The mobile part is composed of magnetic blocks. Both the permanent magnets and the winding are fixed on the stator.

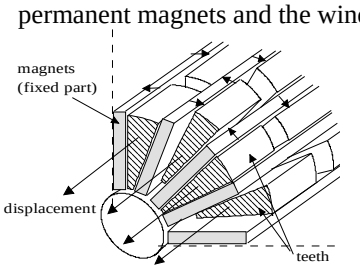

Fig 18a) Composition of the active part of the actuator

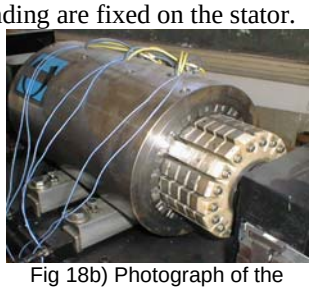

Fig 18b) Photograph of the actuator [designed by LESIR and manufactured by Radio-Energy]

Fig. 18: Example of permanent magnet reluctance multi-airgap actuator

The structure contains 36 airgap surfaces. The path is 55 mm long with a tooth step of 13 mm. When operating in impulse mode (i.e. without any heat limit), this actuator generates a thrust of 24,000 N. The airgap is equal to 1.2 mm and the active volume is 9.6 dm^3, for a peak force-volume ratio of 2,500 N/dm^3.

VII. CONCLUSION

In this paper, a comparison of the evolution in force density as a function of actuator volume for various types of linear actuator architecture has been conducted. The study has served to highlight the advantage of multiplying the number of airgap surfaces in the case of global coil architecture.
An example of an actuator featuring an original design and a high force -volume ratio was also presented.

These results still depend however upon the mechanically feasible rate of active zone splitting. As such, the obstacles involved in this development process merit specific mention, namely:

- the production of magnetic blocks and small-sized magnets, including their assembly;
- mecanical precision to have a small mechanical gap in comparison with the structure's overall dimensions;
- guidance of several mobile parts over long paths;
- compensation for the high normal bonding stresses associated with the eccentricity of mobile parts with respect to fixed parts.

VIII. REFERENCES

[1] Rioux C., « Théorie générale comparative des machines électriques établie à partir des équations du champ électromagnétique », *R.G.E.* - May 1970 - Tome 79, N° 5, pp. 415-421.

[2] Rioux C., « Aspects préliminaires de la théorie des machines électriques comportant des matériaux ferromagnétiques », *Rev. Phys. Appl*., 15, October 1980, pp. 1505-1515.

[3] Ben Ahmed H., Prévond L., Multon B., Salamand B., Lucidarme J., "Special Synchronous Linear Actuators: Structures and Performances", *Revue Electromotion*, 1998

[4] Desesquelles P.F., Lucidarme J., Ben Ahmed H., "Theoretical and Experimental Results Upon Multi-Airgap Axial Synchronous Machines With Permanent Magnets", *ICEM'90*, Cambridge Mass. (USA), August 1990.

[5] Amiet M., Lucidarme J., « Accélérateur ou actionneur linéaire », *French patent, filed by the State*, N° 95 15703, December 1995.

[6] Matt, R. Goyet, J. Lucidarme, C. Rioux, "Longitudinal Field Multi-Airgap Linear Reluctance Actuator", *Electric Machines & Power Systems*, 1987, 13:299-313.

[7] Matt, J.F. Libre, « Performances comparées des machines à aimants et à réluctance variable. Maximisation du couple massique ou volumique », *Journal de Physique* III, October 1995, pp. 1621-1641.

[8] R. Michaux, P. Letellier, « Les machines discoïdes à champ axial dans les systèmes de propulsion électrique », *REE* n°3, March 1997, pp. 37-42.